Published in final edited form as:
Nat Cell Biol. 2009 January ; 11(1): 56–64. doi:10.1038/ncb1812.

MG53 nucleates assembly of cell membrane repair machinery

Chuanxi Cai[1], **Haruko Masumiya**[2], **Noah Weisleder**[1], **Noriyuki Matsuda**[3], **Miyuki Nishi**[2,4], **Moonsun Hwang**[1], **Jae-Kyun Ko**[1], **Peihui Lin**[1], **Angela Thornton**[1], **Xiaoli Zhao**[1], **Zui Pan**[1], **Shinji Komazaki**[5], **Marco Brotto**[1], **Hiroshi Takeshima**[2,4,6], and **Jianjie Ma**[1,6]

[1] Department of Physiology and Biophysics, Robert Wood Johnson Medical School, 675 Hoes Lane, Piscataway, NJ 08854, USA

[2] Department of Medical Chemistry, Graduate School of Medicine, Tohoku University, Japan

[3] Center Laboratory of Frontier Science, The Tokyo Metropolitan Institute of Medical Science, Japan

[4] Department of Biological Chemistry, Kyoto University Graduate School of Pharmaceutical Sciences, Kyoto 606-8501, Japan

[5] Department of Anatomy, Saitama Medical School, Saitama 350-0495, Japan

Abstract

Dynamic membrane repair and remodelling is an elemental process that maintains cell integrity and mediates efficient cellular function. Here we report that MG53, a muscle-specific tripartite motif family protein (TRIM72), is a component of the sarcolemmal membrane-repair machinery. MG53 interacts with phosphatidylserine to associate with intracellular vesicles that traffic to and fuse with sarcolemmal membranes. Mice null for MG53 show progressive myopathy and reduced exercise capability, associated with defective membrane-repair capacity. Injury of the sarcolemmal membrane leads to entry of the extracellular oxidative environment and MG53 oligomerization, resulting in recruitment of MG53-containing vesicles to the injury site. After vesicle translocation, entry of extracellular Ca^{2+} facilitates vesicle fusion to reseal the membrane. Our data indicate that intracellular vesicle translocation and Ca^{2+}-dependent membrane fusion are distinct steps involved in the repair of membrane damage and that MG53 may initiate the assembly of the membrane repair machinery in an oxidation-dependent manner.

To maintain cellular homeostasis, eukaryotic cells must conserve the integrity of their plasma membrane through active recycling and repair in response to various sources of damage[1]. Defects in the intrinsic membrane repair response have been linked to numerous disease states, including muscular dystrophy, heart failure and neurodegeneration[2–5]. Repair of plasma membrane damage requires recruitment of intracellular vesicles to injury sites[6,7]. One protein that has been linked to membrane repair in skeletal muscle is dysferlin[8–10], which is thought to act as a fusogen that participates in restoration of sarcolemmal membrane integrity following muscle injury. Evidence for this role of dysferlin comes, in part, from studies showing that ablation of dysferlin in mice results in muscular dystrophy[8].

Repair of damage to the plasma membrane is an active and dynamic process that requires several steps, including participation of molecular sensor(s) that can detect acute injury to

[6]Correspondence should be addressed to J.M. or H.T. (maj2@umdnj.edu; takeshim@pharm.kyoto-u.ac.jp).

Note: Supplementary Information is available on the Nature Cell Biology website.

COMPETING FINANCIAL INTERESTS

The authors declare no competing financial interests.

the plasma membrane, nucleation of intracellular vesicles at the injury site and vesicle fusion to enable membrane patch formation. It is well demonstrated that entry of extracellular Ca^{2+} is involved in the fusion of intracellular vesicles to reseal the injured plasma membrane[6,11,12], whereas the molecular machinery involved in sensing the damaged membrane signal and the nucleation process for repair-patch formation have not been fully resolved.

We have previously established an immunoproteomic approach that allows identification of proteins involved in myogenesis, Ca^{2+} signalling and maintenance of membrane integrity in striated muscle[13–15]. Here we report isolation of MG53, a muscle-specific tripartite motif family protein (TRIM72), from our immunoproteomic library[16]. We present evidence to show that MG53 is an essential component of the acute membrane repair process by nucleating the assembly of the repair machinery at injury sites.

RESULTS

MG53 is a muscle-specific TRIM family protein

During screening of a previously established immuno-proteomic monoclonal antibody (mAb) library that targets proteins present in striated muscle cells[13–16], we identified an antigen recognized by mAb5259 with a relative molecular mass of 53,000 (M_r 53K). The protein, named mitsugumin53 (MG53), was purified from rabbit skeletal muscle by a mAb5259 immunoaffinity column and subjected to amino acid sequencing. DNA cloning and database searches revealed the primary structure of MG53 in animal species (Supplementary Information, Fig. S1) and the corresponding *mg53* gene at the human *16p11.2* locus. Domain homology analysis revealed that MG53 is a TRIM72, as it contains the prototypical tripartite motif that includes Ring, B-box and coiled-coil moieties[17,18], as well as a SPRY domain at the carboxy terminus[19] (Fig. 1a). RNA hybridization and western blotting demonstrated that MG53 is exclusively expressed in cardiac and skeletal muscle (Fig. 1b; Supplementary Information, Fig. S2). Thus, MG53 is a muscle-specific TRIM family protein.

Progressive muscle pathology in mice with genetic ablation of MG53

To study the physiological function of MG53, we generated a mouse model with targeted deletion of MG53 expression (Fig. S2). The $mg53^{-/-}$ mice are viable until at least 11 months of age under unstressed conditions, and develop progressive muscle pathology with age (Fig. 1c). An increased number of central nuclei and decreased diameter of muscle fibres were observed in skeletal muscle isolated from the older $mg53^{-/-}$ mice (10–11 months), compared with younger $mg53^{-/-}$ mice (3–5 months) and wild-type littermates (Fig. 1d). Younger $mg53^{-/-}$ mice had limited defects in muscle contractility after membrane injury induced by eccentric muscle contraction during a single round of downhill running exercise, whereas contractile function of skeletal muscle was severely compromised in the older $mg53^{-/-}$ mice (Fig. 1e). Insults known to disrupt the plasma membrane[20,21] exacerbated damage in $mg53^{-/-}$ muscle, where weaker and unstable contractile function was observed, compared with the wild-type muscle (Fig. 1f). A striking phenotype of the $mg53^{-/-}$ mice was revealed when the animals were subjected to repeated cycles of downhill running. During the acclimatization period, $mg53^{-/-}$ performed as well as the wild-type in the early days. However, there was a decline in their running times in later days (Supplementary Information, Fig. S3). When stress testing was performed, the $mg53^{-/-}$ mice could not sustain a 20 m min^{-1} running speed, whereas the wild-type mice could run for the full duration of the experiment (Supplementary Information, Movie 1).

Injection of Evans blue dye into mice directly monitors the degree of membrane injury after downhill running[8,22]. Tibialis anterior muscle sections from the *mg53*$^{-/-}$ mice showed significantly more Evans blue staining, compared with the wild-type muscle (Fig. 1g), revealing extensive exercise-induced muscle damage. Quantitative assay of total absorbance of Evans blue extracted from gastrocnemius muscle bundles provides direct support for the increase in muscle damage in the *mg53*$^{-/-}$ mice after downhill running (Fig. 1h). These data show that genetic ablation of MG53 leads to progressive muscle pathology, compromised exercise capacity and increased susceptibility to membrane injury. The severity of these phenotypes seems to be uncovered by eccentric exercise, which greatly increases the need for membrane repair[20]. Although muscle pathology increases when physiological levels of stress are applied during ageing or exercise, a milder phenotype is observed in young, unexercised *mg53*$^{-/-}$ animals. Further investigation is necessary to determine whether adaptive changes in muscle development or the activity of genes homologous to MG53 may partially compensate for the loss of MG53 activity in *mg53*$^{-/-}$ mice.

Defective membrane repair function in *mg53*$^{-/-}$ muscle

To directly evaluate the membrane repair capacity of the *mg53*$^{-/-}$ muscle, we applied an approach used previously[1,8] to measure FM1-43 fluorescent dye entry after laser-induced damage to muscle fibres isolated from 10–11-month-old mice. The wild-type muscle could effectively reseal sarcolemmal membranes, as they showed only minimal FM1-43 entry after laser damage (Fig. 2a). In contrast, significant entry of FM1-43 fluorescent dye into the *mg53*$^{-/-}$ muscle fibres could be observed after laser-induced damage (compare Supplementary Information, Movie 2 with Movie 3), revealing a defective membrane repair function of the *mg53*$^{-/-}$ muscle (Fig. 2b).

Defective membrane repair capacity was also observed with primary myotube cultures from *mg53*$^{-/-}$ neonates that were exposed to mechanical damage caused by penetration of a microelectrode into the sarcolemma membrane (Fig. 2c). Wild-type myotubes could effectively reseal multiple penetrations and survive, whereas the *mg53*$^{-/-}$ myotubes could not recover from such damage and would contract due to Ca^{2+} entry (Fig. 2d; compare Supplementary Information, Movie 4 with Movie 5).

MG53 facilitates repair of acute membrane damage in muscle cells

MG53 was frequently observed to concentrate at the site of injury in adult muscle fibres that were damaged during the isolation procedure (Fig. 3a), further suggesting that this protein participates in repair of muscle membrane damage. To monitor the cellular function of MG53, we expressed a GFP–MG53 fusion protein in *mg53*$^{-/-}$ myotubes and found that GFP–MG53 localized to both the sarcolemmal membrane and intracellular vesicles (Fig. 3b), which is similar to the immunostaining pattern of native MG53 in skeletal muscle (Fig. S4). A similar pattern of membrane association was also observed in C2C12 myogenic cells[23], where live-cell fluorescence imaging revealed vesicular trafficking and plasma membrane fusion events in C2C12 cells transfected with GFP–MG53 (Supplementary Information, Fig. S5a, Movie 6).

Given the phenotype of the *mg53*$^{-/-}$ mouse and the dynamic membrane trafficking properties of MG53, we tested whether MG53 could mediate membrane-patch formation to facilitate repair of acute membrane damage. Mechanical injury of the cell led to rapid recruitment of GFP–MG53-containing vesicles towards the damage site for repair-patch formation (Fig. 3b; Supplementary Information, Movie 7). Similarly, extensive scrape-wounding of C2C12 myotubes also resulted in dense accumulation of GFP–MG53 at the healing site (Supplementary Information, Fig. S5b, Movie 8).

Although live-cell imaging revealed the rapid translocation of GFP–MG53 towards injury sites on the sarcolemma, resolution of individual vesicles requires ultrastructural examination. After a single round of downhill running to induce global damage to the sarcolemmal membrane, muscle preparations rapidly fixed for electron microscopy revealed recruitment of vesicles to the sarcolemma throughout the whole wild-type muscle fibre (Fig. 3c). In contrast, muscle from *mg53*$^{-/-}$ mice showed limited recruitment of vesicles to the damaged sarcolemma (Fig. 3c). These data provide direct evidence that MG53 is necessary for vesicle translocation during muscle membrane repair.

MG53 nucleates recruitment of intracellular vesicles at injury sites in an oxidation-dependent manner

Our next step towards understanding the mechanism of MG53 function in membrane repair involved generation and purification of recombinant MG53 protein for biochemical and molecular studies. Biochemical assays showed that MG53 exists primarily as monomers in a reduced environment, generated by the addition of dithiothreitol (DTT; Fig. 4a). Interestingly, oligomerization of MG53 was observed in the absence of DTT, with only a minor fraction existing in the monomeric form (Fig. 4a, b). Given that the extracellular environment is oxidized relative to the intracellular environment, we hypothesize that acute disruption of the plasma membrane would lead to exposure of the cell interior to the external oxidized environment, and changes in the oxidation state of MG53 may be a signal to activate the acute membrane-repair process. In support of this hypothesis, inclusion of DTT (5 mM) in the extracellular solution produced marked effects on the MG53-mediated membrane repair process in C2C12 cells (Fig. 4c; Supplementary Information, Movie 9). In the presence of a reduced extracellular environment, translocation of GFP–MG53 towards the injury site was largely disrupted (Fig. 4f). Furthermore, addition of micromolar concentrations of thimerosal, an oxidizing agent, to the extracellular solution led to acceleration of GFP–MG53 translocation towards damage sites after injury to the cell (Fig. 4d, f).

As thimerosal oxidizes sulphhydryl groups at cysteine residues, these findings indicate a mutagenesis target to assist in identifying specific amino acids that underlie oxidation-mediated oligomerization of MG53. Mutational scanning of all 16 cysteine residues in MG53 by converting each into alanine revealed one particular mutation, C242A, resulted in complete loss of MG53 oligomerization, even in the absence of DTT (Fig. 4a). Although GFP–C242A maintained membrane targeting, there was complete disruption of its ability to facilitate membrane repair (Fig. 4e), that is, no accumulation of C242A was observed at the injury site (Supplementary Information, Movie 10). All other conserved cysteine mutants formed oligomers under oxidized conditions (data not shown). For example, C313A maintained oxidation-induced oligomerization (Fig. 4a) and showed similar translocation and membrane-repair function as the wild-type GFP–MG53 (Fig. 4g). Similar results were observed in C2C12 myotubes (Supplementary Information, Fig. S6), suggesting that oxidative entry may have a role in the native muscle fibres. To test whether this is the case, we treated intact wild-type skeletal muscle fibres with DTT and observed a significant defect in restoration of sarcolemma integrity following UV laser injury (Fig. 4h). Together, our data suggest that MG53 may react to the entry of an oxidative milieu at residue Cys 242 and form an oligomeric complex that nucleates membrane patch assembly. Formation of an oligomeric complex of MG53 probably requires additional motifs that facilitate the assembly of native MG53 monomers (Supplementary Information, Fig. S7).

Dominant-negative C242A mutation compromises MG53 function in membrane repair

Direct support for MG53-mediated repair-patch formation and restoration of acute sarcolemma membrane damage is shown in Fig. 5, where entry of FM4-64, a red-shifted

variant of FM1-43, was used as an index of membrane repair capacity in *mg53*$^{-/-}$ myotubes transfected with GFP–MG53 or GFP–C242A. After UV-bleaching of the green fluorescence, rapid translocation of GFP–MG53 occurred at the injury site, whereas GFP–C242A remained static due to its defective oligomerization properties (Fig. 5a). Significantly less entry of FM4-64 was observed in cells transfected with GFP–MG53, compared with GFP–C242A (Fig. 5b), suggesting that the mutant was not able to restore membrane integrity following injury (Fig. 5c).

To further test the contribution of MG53 to the membrane repair function in native adult skeletal muscle fibres, we used electroporation-mediated delivery of plasmid DNA containing GFP–MG53 or GFP–C242A into flexor digitorum brevis (FDB) muscle of living wild-type mice. As observed in other studies[24], high efficiency transfection could be achieved with this methodology (Supplementary Information, Fig. S8). Interestingly, in FDB muscle fibres isolated after the muscle recovered from electroporation, GFP–MG53 would often concentrate at the ends of fibres that resealed after enzymatic disassociation of the muscle bundle. In contrast, the GFP–C242A mutant did not appear at these sites of membrane resealing (Fig. 5d). When isolated fibres were assayed for FM4-64 entry after UV damage, elevated dye entry was observed in fibres expressing GFP–C242A, compared with those expressing GFP–MG53 (Fig. 5e). This result suggests that GFP–C242A has a dominant-negative function over the native MG53 membrane repair activity in these wild-type muscle fibres (Fig. 5f), and further supports that oxidation-mediated oligomerization of MG53 is involved in repair-patch formation.

MG53 binds to phosphatidylserine to mediate vesicle accumulation at injury sites

Lipid profiling[25] revealed that recombinant MG53 could interact with phosphatidylserine, a lipid that preferentially appears at the inner leaflet of the plasma membrane and the cytoplasmic face of intracellular vesicles[26] (Fig. 6a). If this interaction allows MG53 to tether to intracellular membranes, then vesicular accumulation following membrane disruption could be monitored by the movement of annexin-V, a protein known to interact with phosphatidylserine[27]. Co-expression of annexin-V–GFP and RFP–MG53 in C2C12 cells showed parallel increases of annexin-V- and MG53-positive membranes at the site of microelectrode penetration (Fig. 6b, c; Supplementary Information, Movie 11). Dense colocalization of annexin-V–GFP and RFP–MG53 was clearly observed at the cell injury site (Fig. 6c), reflecting that MG53 can interact with phophatidylserine and facilitate phosphatidylserine-containing vesicle trafficking to sites of membrane injury.

Labelling of the cell injury-induced vesicle translocation by annexin-V–GFP requires the presence of Ca^{2+} in the extracellular solution, as removal of extracellular (Ca^{2+}_o) abolished the elevation of annexin-V–GFP fluorescence at the cell injury site (Fig. 6d). This is expected, because annexin-V binding to phophatidylserine is dependent on the presence of Ca^{2+} (ref. [27]). In contrast, accumulation of RFP–MG53 at the injury site did not seem to be affected by the removal of Ca^{2+}_o, as the cell injury site remained densely labelled with RFP–MG53 (Supplementary Information, Movie 12). Quantitative analysis showed that although the kinetics of cell injury-induced RFP–MG53 translocation is similar in the presence (Fig. 6c) or absence (Fig. 6e) of Ca^{2+}_o, the steady-state level of RFP–MG53 present at the injury site is reduced in cells bathed in 0 mM Ca^{2+}_o, compared with 2 mM Ca^{2+}_o.

Penetration with a microelectrode can induce focal injury sites, but treatment with low concentrations of saponin can partially permeabilize the plasma membrane. Such treatments induce rapid translocation of GFP–MG53 to the plasma membrane in C2C12 myoblast cells (Fig. 6f). The saponin-induced GFP–MG53 translocation occurred both in the presence or absence of Ca^{2+}_o, suggesting that Ca^{2+}_o entry is not essential for MG53-mediated vesicle translocation towards the cell injury site.

Relative contribution of extracellular Ca^{2+} and oxidation to membrane repair

As Ca^{2+} entry into the cell has been shown to be essential for membrane resealing[5,8], the effect of Ca^{2+}_o entry probably occurs downstream of the MG53-mediated vesicle translocation step during membrane repair. Clearly, removal of Ca^{2+}_o affects the steady-state level of MG53 accumulation at the injury site (Fig. 6e), suggesting that Ca^{2+} entry may potentiate either vesicle trafficking or vesicle fusion, leading to membrane resealing. To test these possibilities, we conducted experiments where the Ca^{2+}_o concentration was rapidly switched from 0 to 2 mM following injury of the cell. Mechanical injury of a *mg53*$^{-/-}$ myotube transfected with GFP–MG53 produced initial translocation of GFP–MG53 to the injury site in the absence of Ca^{2+}_o (Fig. 7a). Rapid perfusion with a Ca^{2+}-containing solution resulted in an additional elevation in GFP fluorescence intensity, and also increased membrane fusion and budding events at the injury sites (Fig. 7b). Quantitative measurements reveal both a Ca^{2+}-dependent and independent component of GFP–MG53 translocation to injury sites in C2C12 cells or *mg53*$^{-/-}$ myotubes (Fig. 7c). Independently of the pre-exposure to 0 Ca^{2+}, the same steady-state GFP–MG53 signal at the injury sites can be observed in cells switched from 0 to 2 mM Ca^{2+}_o as those that are in 2 mM Ca^{2+}_o for the course of the experiment.

To further test the contribution of Ca^{2+} entry and oxidation to plasma membrane resealing in skeletal muscle, we conducted UV-laser wounding assays with individual FDB muscle fibres and monitored the entry of FM1-43 to provide an index of the membrane repair capacity. Wild-type muscle showed effective resealing after UV-induced injury in an extracellular solution containing 2 mM Ca^{2+}_o (Fig. 7d), preventing entry of FM1-43 into the muscle fibre. Removal of Ca^{2+} from the extracellular solution led to marked enhancement of FM1-43 entry, due to the lack of membrane resealing. Interestingly, addition of 10 mM DTT to the 0 Ca^{2+}_o solution caused a further increase in FM1-43 dye entry in wild-type muscle fibres (Fig. 7d). Elevated FM1-43 dye entry was observed in *mg53*$^{-/-}$ muscle fibres following UV-injury, both in the presence and absence of Ca^{2+}_o, and the degree of membrane repair defects was similar under both conditions (Fig. 7e). The extent of FM1-43 dye entry in *mg53*$^{-/-}$ muscle was nearly identical to that of the wild-type muscle bathed in 0 Ca^{2+}_o and 10 mM DTT. These results suggest that the fundamental defect in membrane repair of the *mg53*$^{-/-}$ muscle is likely to be upstream of the Ca^{2+}-dependent membrane resealing process.

DISCUSSION

In this study, we provide evidence that MG53 nucleates assembly of the cell membrane repair machinery at injury sites in muscle cells. Our study further reveals that MG53 is an essential component of the muscle membrane repair machinery, as illustrated by the significant deficiency in membrane repair function of the *mg53*$^{-/-}$ muscle. The response of MG53-mediated membrane patching is rapid, occurring in the order of seconds after injury, indicating that MG53 mediates the acute repair process following cellular damage. We show that the entry of Ca^{2+}_o and exposure to the external oxidized milieu both contribute to the membrane resealing process. In muscle cells, MG53 mediates trafficking to and nucleation of intracellular vesicles at injury sites. This process is driven by changes in the intracellular oxidative environment and does not require Ca^{2+}_o entry to occur. Rather, Ca^{2+}_o entry facilitates vesicle fusion with the plasma membrane to complete the formation of a repair patch. Thus, the repair process on acute membrane damage in muscle requires three distinct steps (Fig. 8). First, the initial membrane damage signal is the exposure of the reduced intracellular environment to the oxidized extracellular milieu, which is sensed by MG53. Second, the oxidation-dependent oligomerization of MG53 nucleates formation of a repair complex through tethering to phosphatidylserine on intracellular vesicles and the inner

leaflet of the plasma membrane. Third, local elevation of Ca^{2+} enables fusion of vesicles with the plasma membrane for formation of a repair patch.

We showed that a conserved cysteine residue (Cys 242) is essential for oxidation-mediated oligomerization of MG53, and is crucial for the MG53-regulated membrane repair function. Moreover, oligomerization of MG53 seems to be an essential step in the acute membrane repair process, as overexpression of GFP–C242A in native skeletal muscle resulted in a significant defect in the membrane repair capacity, possibly due to a dominant-negative effect of the mutant MG53 over the wild-type MG53. Previous studies by several groups provide conclusive evidence that entry of Ca^{2+}_o across the damaged plasma membrane contributes to membrane resealing by facilitating Ca^{2+}-dependent exocytotic membrane fusion events[11,12]. However, if the cell were strictly dependent on increased cytosolic Ca^{2+} to induce vesicle translocation to an injury site, elevation of Ca^{2+} that occurs during normal cellular physiology, such as muscle contraction, could mimic this response and constantly alter vesicle trafficking, or even trigger cell death through excessive Ca^{2+} entry[28]. The lack of selectivity for Ca^{2+} as a signal for vesicle translocation may necessitate that other signals initiate the repair process. Our studies show that changes in the cellular oxidative state could be one such signal in striated muscle.

Acute membrane repair function is particularly important in striated muscle cells, as they must resist the membrane stresses generated by muscle contraction. This may require specific repair processes unique to striated muscle, which is supported by the muscle-specific nature of MG53. Our finding that MG53 is essential for vesicle translocation in striated muscle provides an attractive target for muscle diseases associated with defective membrane repair. Furthermore, a role for oxidative entry-mediated membrane repair in muscle cells would have broad application in both cell biology as well as potential translational impact.

Targeting membrane repair defects is a topic of current interest in the treatment of muscular dystrophy[3,29]. Earlier studies show that dysferlin, another muscle specific protein, has an important role in the maintenance of sarcolemmal membrane integrity. A clear dystrophic phenotype was observed in dysferlin-null mice, and several mutations in the dysferlin gene have been linked to human muscular dystrophy[8,30,31]. It was proposed that dysferlin can function as a fusogen to allow vesicles to form a membrane repair patch[32]. However, it is not known whether dysferlin can facilitate rapid vesicle translocation or can act as a sensor for the membrane repair process, as there have been no live-cell imaging studies that dysferlin itself can facilitate the rapid translocation of vesicles associated with acute membrane damage[10]. Our electron microscopy analysis revealed a clear defect in vesicular accumulation at damaged sarcolemma in *mg53*$^{-/-}$ muscle, whereas *dysferlin*$^{-/-}$ muscle maintained the ability for vesicles to translocation to the sarcolemma[8]. This suggests that although dysferlin may participate in the final membrane resealing process, proteins other than dysferlin are probably required for nucleation of intracellular vesicles towards the acute injury sites. It remains to be established whether MG53 can functionally interact with dysferlin and can therefore facilitate dysferlin function at the plasma membrane during acute membrane repair. Furthermore, future studies are required to test whether MG53 and dysferlin participate in the same or different pathways of the cellular repair process.

It is well known that extensive remodelling of the sarcolemmal membrane and the muscle cell itself occurs in response to activity, trauma, ageing and a variety of pathophysiological conditions. As MG53 is restricted to the cardiac and skeletal muscles, its membrane reparative function provides an entirely new model for potential therapy of muscle and cardiovascular diseases, including muscular dystrophy, cardiomyopathy and age-related muscle wasting.

METHODS

Cloning of MG53 gene, antibody preparation and plasmid construction

The preparation and screening of a mAb library for microsomal proteins of rabbit skeletal muscle, as well as the preparation of mAb5259 (IgG1 subclass) and immunoaffinity purification, was performed as described previously[16]. Purified MG53 was subjected to amino acid sequence analysis and all sequences determined were encoded in the rabbit MG53 cDNA (data not shown). Homology searches in the databases found mouse and human MG53 using the rabbit partial amino acid sequences. An exon region of the mouse MG53 gene was amplified from mouse genomic DNA, and rabbit and mouse skeletal muscle libraries were screened using the ^{32}P-labelled exon fragment to yield full-length cDNAs. A polyclonal antibody against MG53 was raised by injecting an *Escherichia coli*-produced recombinant protein containing residues 145 to 477 of mouse MG53 into rabbits and collecting the resulting serum using standard techniques. Specificity was confirmed by western blotting result in comparison with mAb5259.

GFP–MG53 was constructed by inserting mouse MG53 cDNA into pEGFP-C1 (Invitrogen) plasmid using *Xho*I and *Xba*I. MG53 mutants C242A and C313A were constructed by replacing the appropriate cysteine in GFP–MG53 with alanine using methods described previously[34]. cDNA for annexin-V was amplified from the mouse tissue and subcloned into the pEGFP-N1 plasmid to generate the annexin-V–GFP construct.

Membrane repair assay and *in vivo* muscle transfection

Knockout mice lacking MG53 were generated using our standard methods[13,35] (Supplementary Information, Fig. S2). Myoblasts were isolated from neonatal pups using our established protocols[36] and allowed to differentiate into myotubes for 3–5 days before use. For *in vivo* transfection of adult skeletal muscle with GFP–MG53 and GFP–C242A, 20 μg of plasmid DNA was injected into flexor digitorum brevis (FDB) muscle and acupuncture needles (Millennia) were inserted longitudinally through the mouse foot to allow application of 20 pulses of a100 V cm^{-1} electrical field at 0.1 Hz[24]. Experiments were performed 7 days after electroporation to allow for recovery from any damage generated during experimental manipulations. To isolate FDB muscle fibres, male *mg53*$^{-/-}$ mice, or age-matched wild-type control mice and those transfected with GFP–MG53 were killed by cervical dislocation. FDB muscles were surgically removed in a Tyrode solution containing 140 mM NaCl, 5 mM KCl, 2.5 mM $CaCl_2$, 2 mM $MgCl_2$ and 10 mM HEPES (pH 7.2). Muscles were digested in the same solution supplemented with type I collagenase (2 mg ml^{-1}; Sigma), for 120 min at 37 °C. After collagenase treatment, FDB fibres were dissociated by several passages through a series of pipettes with decreasing diameter[33]. Fibres were plated onto ΔTC3 glass-bottomed dishes (Bioptechs) in Tyrode solution. To avoid potential complications from protein overexpression and aggregation associated with electroporation-mediated transfection of GFP–MG53 and GFP–C242A, only fibres that had comparable levels of GFP signal without apparent aggregation were used for membrane repair assessment. To induce damage to the muscle fibre, a 5 × 5 pixel area of the plasma membrane was irradiated at maximum power (Enterprise, 80 mW, 351/364 nm) for 5 s using a Zeiss-LSM 510 confocal microscope equipped with a ×63 water immersion lens (N.A. 1.3), with 2.5 μM FM1-43 or FM4-64 dye (Molecular Probes) present in the extracellular Tyrode solution. Images were captured at 5 s intervals. For experiments with rapid switching of Ca^{2+}_o, cells were initially bathed in Tyrode solution containing either 2 mM or 0 mM Ca^{2+}_o (plus 0.5 mM EGTA) and at indicated times, cells were perfused by a gravity-flow custom-assembled perfusion system. In experiments where saponin was used to disrupt the cell membrane, Tyrode including 0.005% saponin (Sigma) was perfused as well. For each image, the mean fluorescence intensity was measured with Zeiss LSM 510 imaging

software. To calculate the fluorescence intensity, we used an area of about 200 μm^2 for FM1-43, FM4-64 dye entry, or about 100 μm^2 for GFP or RFP fluorescent intensity, directly adjacent to the injury site. To allow for statistical analysis from different experiments, data is presented as fluorescence intensity relative to the value before injury ($\Delta F/F0$).

Confocal imaging and immunostaining of MG53

To monitor intracellular trafficking of fluorescent fusion proteins, C2C12 cells or *mg53*$^{-/-}$ myotubes were cultured in glass-bottom dishes (Bioptechs) and transfected with plasmid DNA using standard techniques. For immunocytochemistry, FDB fibres were fixed using 100% ethanol at −20 °C for 5 min before anti-mouse MG53 rabbit polyclonal antibody was applied at a 1:200 dilution. Cells were washed and secondary antibodies coupled with fluorescent probes (goat anti-rabbit Alexa Fluor 488 or Alexa Fluor 546) were applied according to the manufacturer's instructions (Molecular Probes). For the assay of acute live-cell membrane damage, transfected cells were mechanically damaged using a micropipette attached to a micromanipulator. Fluorescence images were captured using a BioRad 2100 Radiance laser scanning confocal microscope with a ×40 1.3NA oil immersion objective.

Muscle histology, ultrastructure and contractile function

1% Evans blue dye (10 ml kg^{-1} body weight, Sigma) was injected into the intraperitoneal space of *mg53*$^{-/-}$ or wild-type control mice (10–11 months old) 8–16 h before exercise training. Mice were made to run on an Exer-6M treadmill (Columbus Instruments) on a 15° downhill angle at 8.8 m min^{-1}. for 45 min. After exercise, animals were immediately killed by cervical dislocation and muscles were surgically excised with intact tendons. Contractility measurements were made using established protocols on soleus muscles[33].

Tibialis anterior and extensor digitorum longus (EDL) muscles were either frozen in optimal cutting medium (Sakara) for cryosectioning or fixed overnight in 10% formalin (EMS) at 4 °C for paraffin-embedded sections. Stained sections were examined on an Axiovert 200 microscope (Zeiss). For determination of central nuclei, 16 random sections were counted from 4–8 sections for each mouse (n = 4–8; ref. [37]). Gastrocnemius muscles were split into 2–3 bundles at the tendons, weighed and then soaked in formamide (GibcoBRL) for 48 h at 55 °C with gentle rocking. The optical density of Evans blue in the resulting supernatant was measured at 610 nm with a Spectronic 610 spectrophotometer (Milton Roy). For electron microcopy analysis, animals were killed immediately after the downhill running exercise, and muscles were surgically excised with intact tendons. Muscles were immersed in cold 2.5% glutaraldehyde and processed as described previously[14]. Immunoelectron microscopy using secondary antibody conjugated with 15 nm gold particles was performed essentially as described previously[14].

To determine the effects of multiple cycles of eccentric exercise on *mg53*$^{-/-}$ mice, we adapted previous protocols[8,20], by subjecting the young *mg53*$^{-/-}$ mice (7 months) and their strain- and age-matched wild-type controls to downhill treadmill exercise (4.4 m min^{-1}, 40 min day^{-1} for 3 days, and 4.4 m min^{-1} for 40 min plus 8.8 m min^{-1} for 20 min per day for 8 days to acclimatize to treadmill running, followed by 20 m min^{-1}, 20 min day^{-1} for 2 days to test endurance under stress conditions).

Purification of recombinant MG53 and lipid profiling

Recombinant MG53 protein was purified from *Sf9* cells infected with the Baculovirus Expression System (Pharmingen). 6×His tag was added to the amino terminus of MG53 to allow purification using the Ni-affinity column (Qiagen), according to the manufacture's instructions. MG53 (1 μg ml^{-1}) was applied to PIP_2-Strip membranes (Echelon) according to the manufacture's instructions, using 0.1% milk in PBS as a blocking agent. Western

blots for recombinant MG53 or native MG53 were performed using the anti-mouse MG53 rabbit polyclonal antibody.

Supplementary Material

Refer to Web version on PubMed Central for supplementary material.

Acknowledgments

We thank Michael Reid, Jerome Parness, and Heping Cheng for helpful suggestions to this work. Yi Chu provided assistance in data processing and graphic conversions. We also thank the Cancer Institute of New Jersey Tissue Analytic Services Shared Resource and the UMDNJ-Cell Imaging Core facility, which is supported by NCRR from NIH, for providing assistance with imaging. This work was supported by grants from NIH (J.M.), Ministry of Education, Science, Sports and Culture of Japan (H.T.) and the American Heart Association (C.C., N.W., M.B.).

References

1. McNeil PL, Miyake K, Vogel SS. The endomembrane requirement for cell surface repair. Proc Natl Acad Sci USA 2003;100:4592–4597. [PubMed: 12672953]
2. Doherty KR, McNally EM. Repairing the tears: dysferlin in muscle membrane repair. Trends Mol Med 2003;9:327–330. [PubMed: 12928033]
3. Bansal D, Campbell KP. Dysferlin and the plasma membrane repair in muscular dystrophy. Trends Cell Biol 2004;14:206–213. [PubMed: 15066638]
4. Bazan NG, Marcheselli VL, Cole-Edwards K. Brain response to injury and neurodegeneration: endogenous neuroprotective signaling. Ann NY Acad Sci 2005;1053:137–147. [PubMed: 16179516]
5. McNeil PL, Kirchhausen T. An emergency response team for membrane repair. Nature Rev Mol Cell Biol 2005;6:499–505. [PubMed: 15928713]
6. Steinhardt RA, Bi G, Alderton JM. Cell membrane resealing by a vesicular mechanism similar to neurotransmitter release. Science 1994;263:390–393. [PubMed: 7904084]
7. Miyake K, McNeil PL. Vesicle accumulation and exocytosis at sites of plasma membrane disruption. J Cell Biol 1995;131:1737–1745. [PubMed: 8557741]
8. Bansal D, et al. Defective membrane repair in dysferlin-deficient muscular dystrophy. Nature 2003;423:168–172. [PubMed: 12736685]
9. Towler MC, Kaufman SJ, Brodsky FM. Membrane traffic in skeletal muscle. Traffic 2004;5:129–139. [PubMed: 15086789]
10. Klinge L, et al. From T-tubule to sarcolemma: damage-induced dysferlin translocation in early myogenesis. FASEB J 2007;21:1768–1776. [PubMed: 17363620]
11. Terasaki M, Miyake K, McNeil PL. Large plasma membrane disruptions are rapidly resealed by Ca^{2+}-dependent vesicle-vesicle fusion events. J Cell Biol 1997;139:63–74. [PubMed: 9314529]
12. McNeil PL, Vogel SS, Miyake K, Terasaki M. Patching plasma membrane disruptions with cytoplasmic membrane. J Cell Sci 2000;113:1891–1902. [PubMed: 10806100]
13. Nishi M, et al. Abnormal features in skeletal muscle from mice lacking mitsugumin29. J Cell Biol 1999;147:1473–1480. [PubMed: 10613905]
14. Takeshima H, Komazaki S, Nishi M, Iino M, Kangawa K. Junctophilins: a novel family of junctional membrane complex proteins. Mol Cell 2000;6:11–22. [PubMed: 10949023]
15. Yazawa M, et al. TRIC channels are essential for Ca^{2+} handling in intracellular stores. Nature 2007;448:78–82. [PubMed: 17611541]
16. Weisleder N, Takeshima H, Ma J. Immuno-proteomic approach to excitation-contraction coupling in skeletal and cardiac muscle: molecular insights revealed by the mitsugumins. Cell Calcium 2008;43:1–8. [PubMed: 18061662]
17. Reymond A, et al. The tripartite motif family identifies cell compartments. EMBO J 2001;20:2140–2151. [PubMed: 11331580]

18. Meroni G, Diez-Roux G. TRIM/RBCC, a novel class of 'single protein RING finger' E3 ubiquitin ligases. Bioessays 2005;27:1147–1157. [PubMed: 16237670]
19. Ponting C, Schultz J, Bork P. SPRY domains in ryanodine receptors (Ca^{2+}-release channels). Trends Biochem Sci 1997;22:193–194. [PubMed: 9204703]
20. McNeil PL, Khakee R. Disruptions of muscle fiber plasma membranes. Role in exercise-induced damage. Am J Pathol 1992;140:1097–1109. [PubMed: 1374591]
21. Takekura H, Fujinami N, Nishizawa T, Ogasawara H, Kasuga N. Eccentric exercise-induced morphological changes in the membrane systems involved in excitation-contraction coupling in rat skeletal muscle. J Physiol 2001;533:571–583. [PubMed: 11389213]
22. Coral-Vazquez R, et al. Disruption of the sarcoglycan–sarcospan complex in vascular smooth muscle: a novel mechanism for cardiomyopathy and muscular dystrophy. Cell 1999;98:465–474. [PubMed: 10481911]
23. Pan Z, et al. Dysfunction of store-operated calcium channel in muscle cells lacking mg29. Nature Cell Biol 2002;4:379–383. [PubMed: 11988740]
24. Pouvreau S, et al. Ca^{2+} sparks operated by membrane depolarization require isoform 3 ryanodine receptor channels in skeletal muscle. Proc Natl Acad Sci USA 2007;104:5235–5240. [PubMed: 17360329]
25. Dowler S, Kular G, Alessi DR. Protein lipid overlay assay. Sci STKE 2002;2002:PL6. [PubMed: 11972359]
26. Li D, Miller M, Chantler PD. Association of a cellular myosin II with anionic phospholipids and the neuronal plasma membrane. Proc Natl Acad Sci USA 1994;91:853–857. [PubMed: 8302857]
27. Swairjo MA, Concha NO, Kaetzel MA, Dedman JR, Seaton BA. Ca^{2+}-bridging mechanism and phospholipid head group recognition in the membrane-binding protein annexin V. Nature Struct Biol 1995;2:968–974. [PubMed: 7583670]
28. Dong Z, Saikumar P, Weinberg JM, Venkatachalam MA. Calcium in cell injury and death. Annu Rev Pathol 2006;1:405–434. [PubMed: 18039121]
29. Han R, Campbell KP. Dysferlin and muscle membrane repair. Curr Opin Cell Biol 2007;19:409–416. [PubMed: 17662592]
30. Weiler T, et al. Identical mutation in patients with limb girdle muscular dystrophy type 2B or Miyoshi myopathy suggests a role for modifier gene(s). Hum Mol Genet 1999;8:871–877. [PubMed: 10196377]
31. Saito A, et al. Miyoshi myopathy patients with novel 5′ splicing donor site mutations showed different dysferlin immunostaining at the sarcolemma. Acta Neuropathol 2002;104:615–620. [PubMed: 12410383]
32. Glover L, Brown RH Jr. Dysferlin in membrane trafficking and patch repair. Traffic 2007;8:785–794. [PubMed: 17547707]
33. Weisleder N, et al. Muscle aging is associated with compromised Ca^{2+} spark signaling and segregated intracellular Ca^{2+} release. J Cell Biol 2006;174:639–645. [PubMed: 16943181]
34. Ko JK, Ma J. A rapid and efficient PCR-based mutagenesis method applicable to cell physiology study. Am J Physiol Cell Physiol 2005;288:C1273–C1278. [PubMed: 15659713]
35. Takeshima H, et al. Excitation-contraction uncoupling and muscular degeneration in mice lacking functional skeletal muscle ryanodine-receptor gene. Nature 1994;369:556–559. [PubMed: 7515481]
36. Yang D, et al. RyR3 amplifies RyR1-mediated Ca^{2+}-induced Ca^{2+} release in neonatal mammalian skeletal muscle. J Biol Chem 2001;276:40210–40214. [PubMed: 11500519]
37. Millay DP, et al. Genetic and pharmacologic inhibition of mitochondrial-dependent necrosis attenuates muscular dystrophy. Nature Med 2008;14:442–447. [PubMed: 18345011]

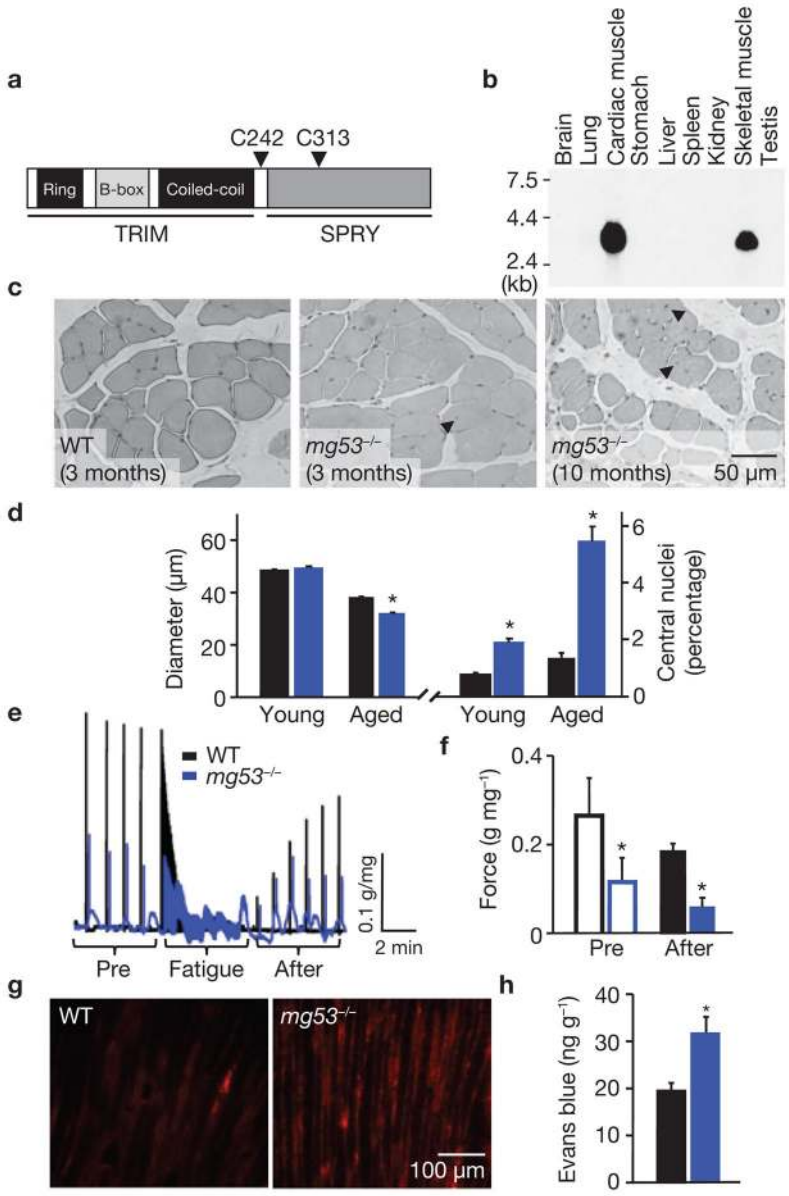

Figure 1.

Mice null for MG53, a muscle specific TRIM family protein, show progressive muscle pathology. (**a**) Motif structure of MG53. For detailed alignment of mouse, rabbit and human protein sequences, see Supplementary Information, Fig. S1. (**b**) Northern blot analysis of mouse tissues shows the specific expression of MG53 in skeletal and cardiac muscles. Total RNA (15 μg per lane) from different mouse tissues was analysed using a cDNA probe following a procedure described previously[14]. (**c**) Haematoxylin and eosin (H&E) staining of EDL muscle sections illustrates the increased number of central nuclei (arrows) in ageing $mg53^{-/-}$ muscle (10 months), compared with young (3 months) wild-type (WT) or $mg53^{-/-}$ mice. (**d**) The diameter of muscle fibres in aged (10–11 months) $mg53^{-/-}$ mice (32.1 ± 0.3 μm, $n = 541$, $^*P < 0.05$ by ANOVA) was decreased, compared with aged (10–11 months) WT controls (37.9 ± 0.5 μm, $n = 562$), whereas there was no difference in young (3–5 months) WT (48.4 ± 0.5 μm, $n = 765$) versus $mg53^{-/-}$ (49.5 ± 0.5 μm, $n = 673$) muscle. Percentage of muscle fibres that with central nuclei in $mg53^{-/-}$ skeletal muscle (5.47 ±

0.01%, *$P < 0.05$, ANOVA) increased with age when compared with WT (1.25 ± 0.00%). Data are mean ± s.e.m. (**e**) Trace recordings of contractile performance of intact soleus muscle obtained from ageing mice subjected to 30 min downhill running was assessed using an *in vitro* voltage stimulation protocol as described previously[33]. The black trace represents WT muscle, blue trace corresponds to $mg53^{-/-}$ muscle. (**f**) Before fatigue stimulation, the maximal tetanic force, normalized in g mg^{-1} total protein, was significantly lower in $mg53^{-/-}$ muscle (0.12 ± 0.05), compared with WT (0.27 ± 0.08, $n = 4$). At 6 min after fatigue stimulation, the WT muscle (0.18 ± 0.02) recovered significantly more than $mg53^{-/-}$ muscle (0.06 ± 0.02, *$P < 0.05$, ANOVA). (**g**) Extensive Evans blue staining reveals severe damage in $mg53^{-/-}$ tibialis anterior muscle subjected to a single round of downhill running, compared with minimal staining in WT muscles. (**h**) Elevated levels of Evans blue dye could be extracted from the gastrocnemius muscle of $mg53^{-/-}$ mice after a single round of eccentric exercise. Data represent mean ± s.d. ($n = 4$), *$P < 0.01$.

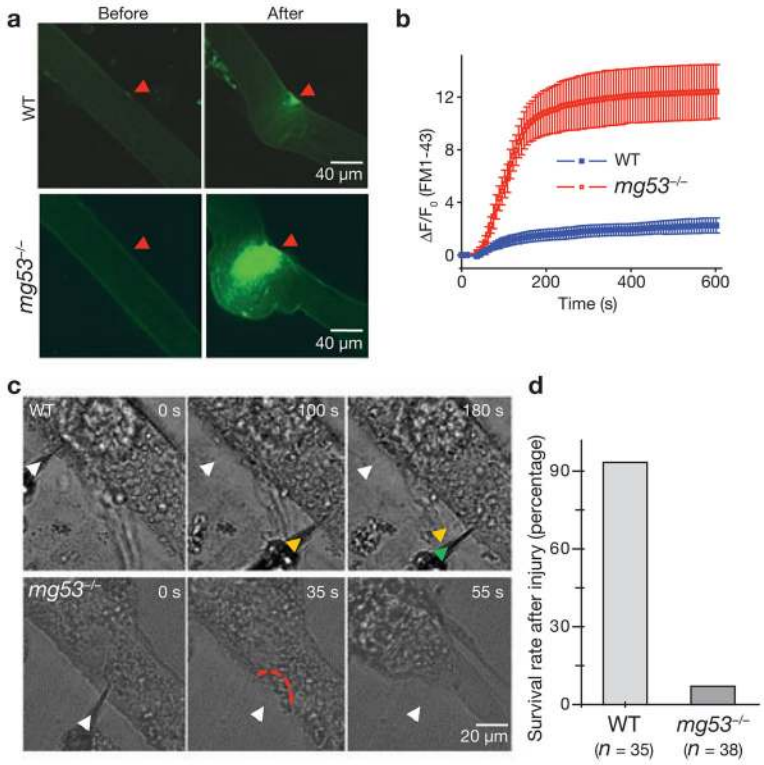

Figure 2.

Defective membrane repair capacity in *mg53*$^{-/-}$ muscle. (**a**) Isolated FDB fibres from ageing WT mice can effectively exclude FM1-43 dye after UV-laser induced damage, whereas fibres from ageing *mg53*$^{-/-}$ mice cannot prevent dye entry. The arrow indicates a wounding site at 401 s after laser injury. Local contraction due to the entry of Ca^{2+}_{o} was greater in *mg53*$^{-/-}$ muscle, and exceeds that reported previously[8]. (**b**) Time-dependent accumulation of FM1-43 inside FDB muscle fibre induced by laser damage of the sarcolemmal membrane with Ca^{2+} present in the extracellular solution. Data are mean ± s.e.m of 30 fibres obtained from WT mice and 18 fibres from *mg53*$^{-/-}$ mice. (**c**) Representative images of differentiated myotubes derived from WT or *mg53*$^{-/-}$ neonates indicate that WT myotubes do not contract after mechanical damage by multiple penetrations with a microelectrode (arrows), whereas *mg53*$^{-/-}$ myotubes contract after a single injury, reflecting their defective membrane-repair capacity. (**d**) As these microelectrode penetration experiments were conducted with Ca^{2+} present in the extracellular solution, the lack of membrane resealing will lead to excessive Ca^{2+} entry and contraction of myotubes. If the cell did not contract over a 5 min period, it was considered to have survived microelectrode injury. The summary data presented indicates that *mg53*$^{-/-}$ muscle has markedly compromised ability to reseal cellular membranes following injury.

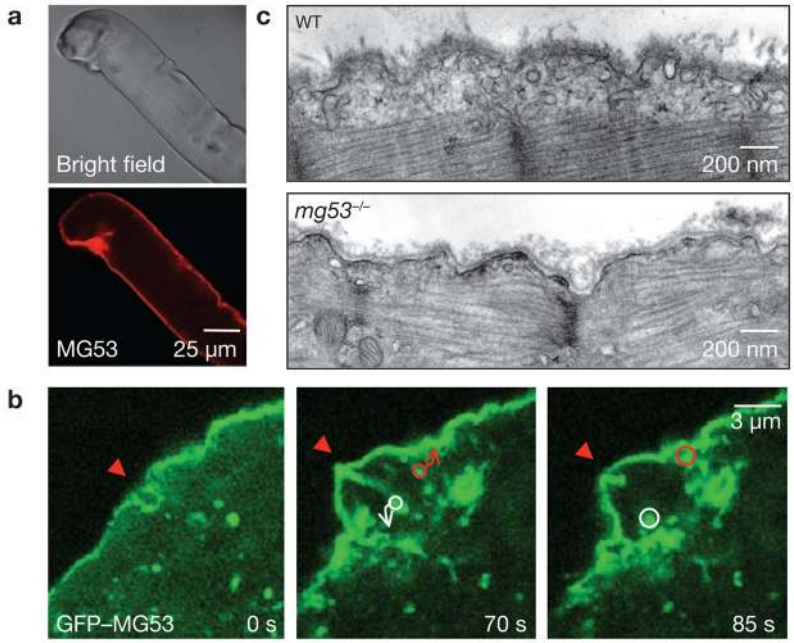

Figure 3.

MG53 facilitates repair of acute membrane damage in muscle cells. (**a**) Immunostaining of MG53 in isolated WT FDB fibres to illustrate the concentration of MG53 at the injury site. These are representative images from more than 20 different muscle fibres that show damage during isolation. (**b**) GFP–MG53 expressed in *mg53*$^{-/-}$ myotubes localizes to intracellular vesicles and sarcolemmal membrane (left). Penetration with a microelectrode leads to accumulation of GFP–MG53 at the injury sites (arrows) at 70 s after injury (right, n = 18). Circles surround individual vesicles containing GFP–MG53 and arrows indicate the path to fusion with the injury site. See Supplementary Information, Movie 7 for visualization of the dynamic process of GFP–MG53 vesicle translocation. (**c**) Representative electron micrographs of EDL muscle following downhill running exercise. Sub-sarcolemmal accumulation of vesicles was observed in 70 out of 79 muscle fibres examined in WT preparations from two different 6-month-old mice. In contrast, *mg53*$^{-/-}$ muscle fibres lack accumulation of intracellular vesicles, as 41 out of 104 muscle fibres from two aged-matched *mg53*$^{-/-}$ animals do not show such accumulation.

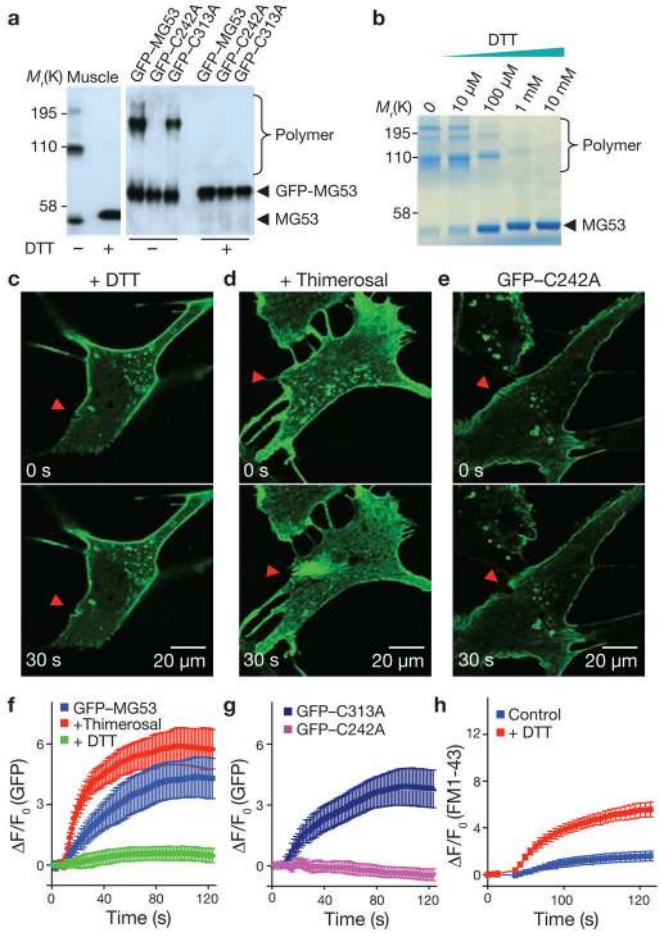

Figure 4.

Oxidation-mediated MG53 oligomerization serves as a nucleation mechanism for acute membrane repair. (**a**) Western blot of mouse skeletal muscle (0.2 μg) or C2C12 cell lysates (0.5 μg per lane) from cells transfected with GFP–MG53, GFP–C242A or GFP–C313A. Native MG53 dimers and tetramers from skeletal muscle were observed under oxidizing condition (–DTT), and after addition of 10 mM DTT (+DTT) caused MG53 to de-oligomerize into the monomeric form (left). The GFP–C242A mutant did not form oligomers, even in the oxidized state, whereas GFP–C313A behaved similarly to WT GFP–MG53 (right; $n = 9$ for skeletal muscle preparation and $n = 8$ for C2C12 cells). (**b**) Purified recombinant MG53 protein shows concentration-dependent de-oligomerization in response to DTT. (**c**) The presence of DTT (5 mM) in the bathing solution of C2C12 cells abolished GFP–MG53 accumulation at injury sites. (**d**) Addition of thimerosal (2 μM) to the extracellular solution accelerated accumulation of GFP–MG53 at the damage site of a C2C12 cell. (**e**) GFP–C242A localized to intracellular vesicles and plasma membrane, but did not accumulate at the microelectrode injury sites. Arrowheads indicate the location of microelectrode penetration (**c**–**e**). (**f**) Time-course of GFP–MG53 accumulation at injury sites following microelectrode penetration in untreated C2C12 cells and in the presence of DTT or thimerosal. Data represent mean ± s.e.m. ($n = 12$). (**g**) Time-course of GFP–C242A and GFP–C313A accumulation at injury sites after microelectrode penetration in C2C12 cells. Data represent mean ± s.e.m. ($n = 15$). (**h**) Time-course of FM1-43 entry into WT skeletal muscle fibres in the presence or absence of DTT (10 mM) following laser induced injury. Data represent mean ± s.e.m. ($n = 8$).

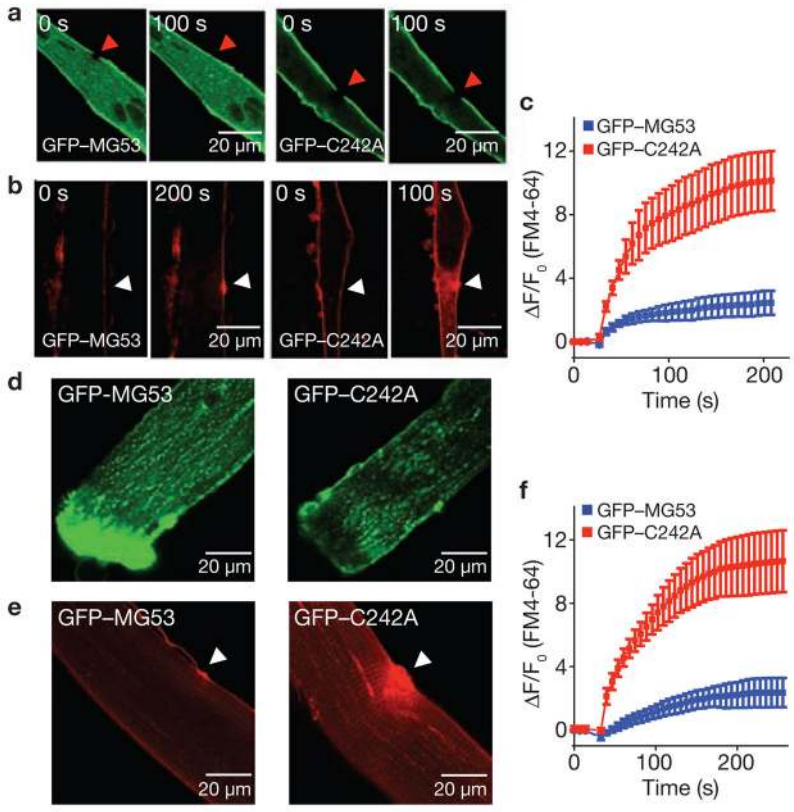

Figure 5.

Repair patch formation by MG53 restores cell integrity following acute injury. (**a**) GFP–MG53 expressed in *mg53*$^{-/-}$ myotubes translocates to cell injury site after UV-bleaching (left), whereas GFP–C242A remains immobile after photobleaching (right). (**b**) *mg53*$^{-/-}$ myotubes transfected with GFP–MG53 (left) or GFP–C242A (right) were assayed for FM4-64 dye entry after UV-laser damage. Arrows indicate the site of laser damage. (**c**) GFP–MG53 expression (blue) can prevent FM4-64 dye entry, whereas GFP–C242A cannot (red). Data represent mean ± s.e.m. (n = 9). (**d**) FDB muscle fibres from WT mice were transfected by *in vivo* electroporation to allow for transient expression of GFP–MG53 (left) and GFP–C242A (right) (see also Supplementary Information, Fig. S5). (**e**) FDB muscle fibres transfected with GFP–C242A show excessive FM4-64 dye entry following UV-laser wounding (right), compared with those transfected with GFP–MG53 (left; n = 15). (**f**) Summary data for panel **e**. Data represent mean ± s.e.m., n = 8.

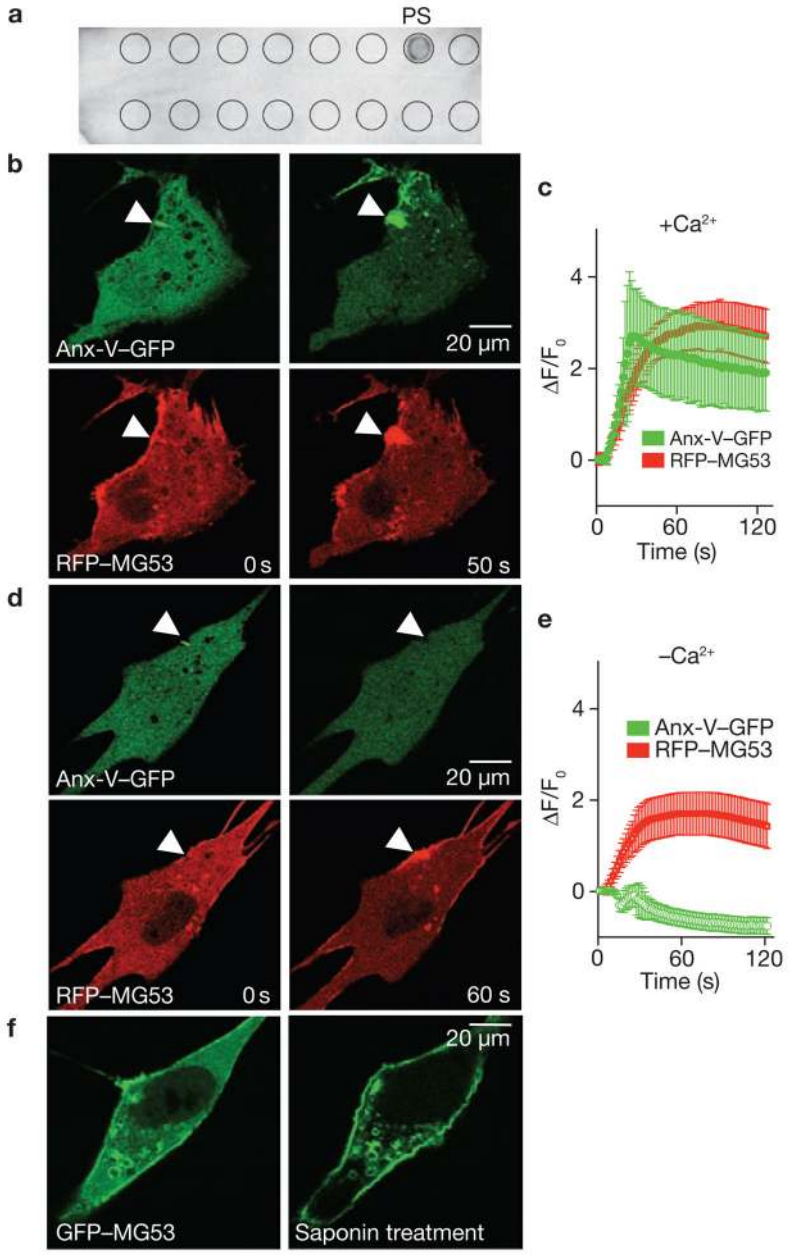

Figure 6.

MG53 binds to phosphatidylserine (PS) to mediate Ca^{2+}-independent vesicle translocation to the injury site. (**a**) PIP_2-Strip lipid dot blot analysis reveals recombinant MG53 (1 μg ml^{-1}) binds PS but not other membrane lipids, including sphingosine-1-P, phosphatidic acid, phosphotidylcholine, phosphatidylethanolamine and various phosphainositol metabolites. (**b**) Microelectrode penetration of C2C12 cells co-expressing annexin-V–GFP (top) and RFP–MG53 (bottom) in the presence of 2 mM Ca^{2+}_o results in colocalization of annexin-V and MG53 at the injury site. (**c**) Time-course of annexin-V–GFP and RFP–MG53 accumulation at injury sites following microelectrode penetration into C2C12 cells. RFP–MG53 continued to accumulate at the injury site, whereas annexin-V–GFP accumulation seemed to be biphasic. Membrane resealing probably reduces Ca^{2+} entry-dependent binding of annexin to PS-enriched membrane surfaces at later time points. Data represent mean ±

s.e.m. (n = 16). (**d**) Removal of Ca^{2+}_o prevents movement of annexin-V–GFP (top) to the injury site (arrow), whereas RFP–MG53 can still translocate following membrane disruption (bottom). (**e**) Time-dependent changes for accumulation of RGP–MG53 and annexin-V–GFP following acute injury of C2C12 cells in the absence of Ca^{2+}_o plus 0.5 mM EGTA. Data represent mean ± s.e.m., n = 12. (**f**) C2C12 myoblasts transfected with GFP–MG53 show translocation of GFP–MG53 to the plasma membrane following treatment with 0.005% saponin in an extracellular solution containing 0 Ca^{2+} plus 0.5 mM EGTA.

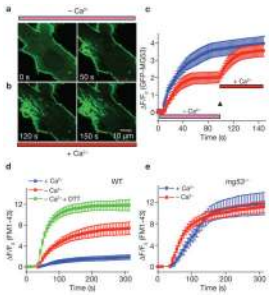

Figure 7.

Relative contribution of extracellular Ca^{2+} and oxidation to membrane repair in skeletal muscle. (**a**) Injury of GFP–MG53 expressing *mg53*$^{-/-}$ myotube by penetration with a microelectrode leads to accumulation of GFP–MG53 at the damage sites in an extracellular solution containing 0 Ca^{2+} and 0.5 mM EGTA (–Ca^{2+}). (**b**) Rapid perfusion of solution containing 2 mM Ca^{2+} (+Ca^{2+}) elevated the accumulation and fusion of GFP–MG53 containing vesicles at the injury site. (**c**) Time-dependent accumulation of GFP–MG53 at the injury sites show a two-step translocation of GFP–MG53 in response to acute damage to the plasma membrane in the absence of Ca^{2+}, followed by addition of 2 mM Ca^{2+} (red), compared with continuous incubation with 2 mM Ca^{2+} for *mg53*$^{-/-}$ myotubes transfected with GFP–MG53 (blue). Data are mean ± s.e.m (n = 12). (**d**) Time-dependent accumulation of FM1-43 dye inside WT muscle fibre induced by a laser damage of the sarcolemmal membrane with the presence of 2 mM Ca^{2+}_o, or absence of Ca^{2+}_o (0 Ca^{2+} plus 0.5 mM EGTA), or incubated with 8 mM DTT and 0.5 mM EGTA in the extracellular solution. Data represent mean ± s.e.m. (n = 12 fibres for each group). (**e**) Time-dependent accumulation of FM1-43 inside *mg53*$^{-/-}$ muscle fibre induced by laser damage of the sarcolemmal membrane with the presence of 2 mM Ca^{2+}_o, or absence of Ca^{2+}_o. Data represent mean ± s.e.m. (n = 12 fibres for each group).

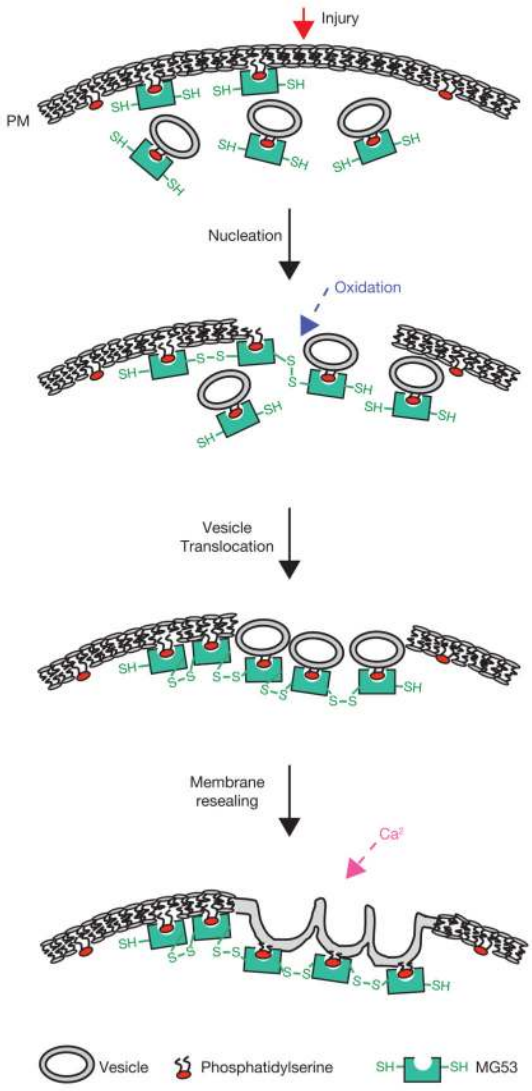

Figure 8.

A schematic representation of the proposed function of MG53 in muscle membrane repair. Through interaction with phosphatidylserine, MG53 is tethered to plasma membrane and intracellular vesicles in cells with intact plasma membrane. Upon membrane damage, entry of the oxidized milieu of the extracellular space into the reduced environment within the cell results in oligomeriztion of MG53 at the injury site. This oligomerization acts as a nucleation site for recruitment of MG53-tethered intracellular vesicles toward the injury site. Local elevation of intracellular Ca^{2+} at the injury site facilitates fusion of intracellular vesicles with the plasma membrane to reseal the damaged membrane.